

Mitigating Visual Knowledge Forgetting in MLLM Instruction-tuning via Modality-decoupled Gradient Descent

Junda Wu
juw069@ucsd.edu
UC San Diego
La Jolla, USA

Yuxin Xiong
y7xiong@ucsd.edu
UC San Diego
La Jolla, USA

Xintong Li
xil240@ucsd.edu
UC San Diego
La Jolla, USA

Yu Xia
yux078@ucsd.edu
UC San Diego
La Jolla, USA

Ruoyu Wang
ruoyu.wang5@unsw.edu.au
University of New South
Wales
Sydney, Australia

Yu Wang
yuw164@ucsd.edu
UC San Diego
La Jolla, USA

Tong Yu
tyu@adobe.com
Adobe Research
San Jose, USA

Sungchul Kim
sukim@adobe.com
Adobe Research
San Jose, USA

Ryan A. Rossi
ryrossi@adobe.com
Adobe Research
San Jose, USA

Lina Yao
lina.yao@unsw.edu.au
University of New South
Wales
Sydney, Australia

Jingbo Shang
jshang@ucsd.edu
UC San Diego
La Jolla, USA

Julian McAuley
jmcauley@ucsd.edu
UC San Diego
La Jolla, USA

Abstract

Recent MLLMs have shown emerging visual understanding and reasoning abilities after being pre-trained on large-scale multimodal datasets. Unlike pre-training, where MLLMs receive rich visual-text alignment, instruction-tuning is often text-driven with weaker visual supervision, leading to the degradation of pre-trained visual understanding and causing visual forgetting. Existing approaches, such as direct fine-tuning and continual learning methods, fail to explicitly address this issue, often compressing visual representations and prioritizing task alignment over visual retention, which further worsens visual forgetting. To overcome this limitation, we introduce a novel perspective leveraging effective rank to quantify the degradation of visual representation richness, interpreting this degradation through the information bottleneck principle as excessive compression that leads to the degradation of crucial pre-trained visual knowledge. Building on this view, we propose a modality-decoupled gradient descent (MDGD) method that regulates gradient updates to maintain the effective rank of visual representations while mitigating the over-compression effects described by the information bottleneck. By explicitly disentangling the optimization of visual understanding from task-specific alignment, MDGD preserves pre-trained visual knowledge while enabling efficient task adaptation. To enable lightweight instruction-tuning, we further develop a memory-efficient fine-tuning approach using gradient masking, which selectively updates a subset of model parameters

to enable parameter-efficient fine-tuning (PEFT), reducing computational overhead while preserving rich visual representations. Extensive experiments across various downstream tasks and backbone MLLMs demonstrate that MDGD effectively mitigates visual forgetting from pre-trained tasks while enabling strong adaptation to new tasks.

Keywords

Visual Knowledge Forgetting, Multimodal Large Language Models

ACM Reference Format:

Junda Wu, Yuxin Xiong, Xintong Li, Yu Xia, Ruoyu Wang, Yu Wang, Tong Yu, Sungchul Kim, Ryan A. Rossi, Lina Yao, Jingbo Shang, and Julian McAuley. 2025. Mitigating Visual Knowledge Forgetting in MLLM Instruction-tuning via Modality-decoupled Gradient Descent. In . ACM, New York, NY, USA, 11 pages. <https://doi.org/10.1145/nnnnnnnn.nnnnnnnn>

1 Introduction

Multimodal large language models (MLLMs) enhanced visual understanding and reasoning by pre-training on large-scale multimodal datasets with comprehensive visual descriptions that integrate textual and visual knowledge [3, 25, 31, 33, 65]. These models achieve strong performance across various vision-language tasks, such as visual question answering [21], multimodal reasoning [19, 63, 70], multimodal recognition [46, 61], personalized multimodality [58], and document intelligence [21, 46]. However, adapting pre-trained MLLMs to downstream tasks via instruction-tuning [24, 26, 33, 43, 57] presents a critical challenge of visual forgetting. Unlike pre-training, where models receive rich visual-text alignment, instruction-tuning is often text-driven with limited direct visual supervision. This shift in training focus leads to the degradation of pre-trained visual encoding [22, 42, 57, 72], negatively impacting model generalizability across downstream tasks that require strong visual knowledge [4, 16]. Addressing this challenge is

Permission to make digital or hard copies of all or part of this work for personal or classroom use is granted without fee provided that copies are not made or distributed for profit or commercial advantage and that copies bear this notice and the full citation on the first page. Copyrights for components of this work owned by others than the author(s) must be honored. Abstracting with credit is permitted. To copy otherwise, or republish, to post on servers or to redistribute to lists, requires prior specific permission and/or a fee. Request permissions from permissions@acm.org.
Conference'17, Washington, DC, USA

© 2025 Copyright held by the owner/author(s). Publication rights licensed to ACM.
ACM ISBN 978-x-xxxx-xxxx-x/YYYY/MM
<https://doi.org/10.1145/nnnnnnnn.nnnnnnnn>

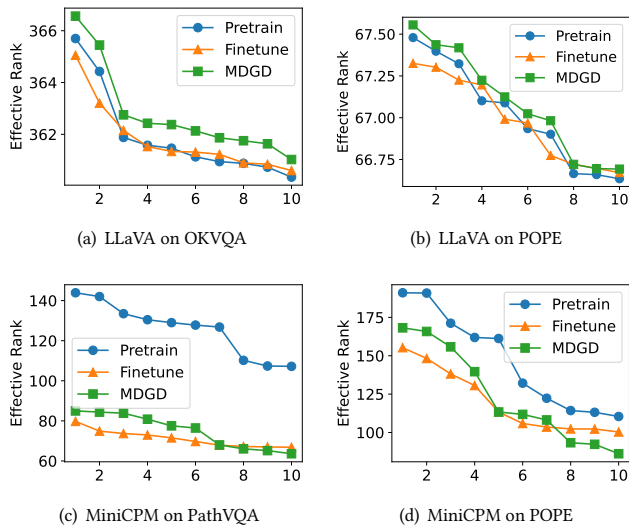


Figure 1: The top-10 image tokens with the highest effective ranks on OKVQA and POPE encoded by LLaVA, and PathVQA and POPE encoded by MiniCPM. We compare pretrained, finetuned, and MDGD-finetuned models. Effective rank [56] quantifies representation richness, and we novelly use it to analyze visual degradation in instruction-tuned MLLMs. Results show that MDGD preserves higher effective rank, mitigating visual forgetting.

essential for ensuring MLLMs retain their visual capabilities while aligning with new tasks efficiently.

While several approaches have attempted to mitigate catastrophic forgetting in neural networks through direct fine-tuning and continual learning methods [47, 62, 71, 73], these methods often overlook the unique challenge of preserving visual knowledge in multimodal large language models (MLLMs). Directly fine-tuning MLLMs on new tasks often leads to overfitting to textual instructions while inadvertently suppressing visual representations [68]. Existing continual learning strategies such as regularization and replay methods tend to focus on retaining language-based knowledge, neglecting the critical trade-off between compressing visual representations and aligning them with task-specific instructions [22, 42, 57, 72], leading to the degradation of pre-trained visual knowledge. Task-orthogonal gradient descent techniques have shown promise in disentangling gradients for multi-task optimization. However, their practical application in MLLMs poses unique challenges. MLLMs are pre-trained on vast and heterogeneous multimodal datasets [3, 25, 31], where it is challenging to precisely isolate task-specific gradients, causing the components critical for visual understanding to become entangled with other features.

To gain a fundamental view of the challenge of visual knowledge forgetting in MLLM instruction tuning, we adopt an information bottleneck (IB) perspective that characterizes the trade-off between retaining input information and ensuring output predictiveness [50]. To investigate the degradation of crucial pre-trained visual knowledge, we introduce a novel perspective that leverages effective rank to quantify the richness of the encoded visual

representation from MLLMs. Specifically, we illustrate the visual forgetting problem in Figure 1, where we observe a consistent effective rank reduction problem caused by MLLM instruction tuning. Based on this view, we propose a modality-decoupled gradient descent (MDGD) method, which disentangles the optimization of visual understanding from task-specific alignment, MDGD regulates gradient updates to maintain the effective rank of visual representations compared with pre-trained MLLMs, while mitigating the over-compression effects described by the information bottleneck. Intuitively, visual forgetting occurs due to the shift from rich multimodal pre-training to instruction-tuning, where text-based supervision dominates without direct visual supervision. By explicitly decoupling the task-specific alignment with visual representation learning, MDGD preserves expressive and robust visual features. To further improve efficiency in instruction-tuning, we introduce a memory-efficient fine-tuning strategy using gradient masking, which selectively updates a subset of model parameters for parameter-efficient fine-tuning (PEFT). This approach reduces computational overhead while ensuring that crucial pre-trained visual representations are retained.

We summarize our contributions as follows:

- We analyze the visual knowledge forgetting problem in MLLM instruction tuning and frame the problem through the lens of effective rank and information bottleneck theory.
- We propose MDGD, which decouples visual optimization from task-specific alignment to preserve visual representations and introduces a PEFT variant MDGD-GM to reduce computational overhead through gradient masking.
- We conduct comprehensive experiments on various MLLMs and downstream tasks, demonstrating that MDGD effectively mitigates visual forgetting while enabling strong adaptation to new tasks.

2 Related Work

2.1 Visual Knowledge Forgetting in MLLMs

Catastrophic forgetting, a persistent challenge in continual learning, occurs when a model forgets previous knowledge while learning new tasks, reducing its performance on earlier tasks [55]. This issue has gained attention in LLMs due to the growing need for continual pre-training and instruction tuning [38, 62]. MLLMs, which integrate multiple modalities through feature encoders projecting inputs into the LLM’s token space, are also prone to catastrophic forgetting [68]. While several methods have attempted to address this issue by adapting continual learning techniques, ranging from fine-tuning and task-orthogonal gradient descent to knowledge distillation and replay-based strategies [47, 62, 71, 73], these approaches often fall short of preserving rich visual representations. For instance, fine-tuning MLLMs on new tasks tends to overfit textual instructions, inadvertently suppressing visual features, and even parameter-efficient adaptations like LoRA have been shown to suffer from forgetting [7, 32]. Model Tailor [73] addresses forgetting by adapting the LLM backbone across reasoning tasks but neglects the critical visual knowledge forgetting problem, which may lead to visual hallucination or deficiency problems while generalizing to various tasks [68]. In contrast, our method offers a more principled and synchronized approach to instruction tuning

that jointly optimizes the alignment between the visual encoder and the LLM, effectively preserving pre-trained visual knowledge while mitigating the degradation of visual representation learning in previous works.

2.2 Information Theory in LLMs

The Information Bottleneck (IB) method [50] in Large Language Models (LLMs) focuses on compressing input data while preserving information relevant to the target output [5, 52, 56, 59]. Previous works employ IB to extract robust task-specific features [60, 69] and enable feature attribution [20, 27]. However such methods focus on information compression in language models [64], while the unique visual knowledge forgetting problem cannot be directly viewed and interpreted. In addition, existing information-theoretic transfer learning methods [29, 51, 60] cannot be directly applied to MLLMs, where the multimodal knowledge is entangled and fused by a dominant LLM. In contrast to these prior works, our approach leverages effective rank to quantify and mitigate the over-compression of visual representations in MLLMs. Specifically, our modality-decoupled gradient descent (MDGD) method explicitly decouples visual optimization from task-specific alignment, which cannot be enabled by existing IB-based methods for LLMs.

3 Preliminary

Task Definition. Given an MLLM π_θ and instruction-tuning dataset D , the image prompt $I \in \Omega$ is encoded by a visual encoder f into a sequence of M visual tokens $f(I) = X^v = (x_1^v, x_2^v, \dots, x_M^v)$. During instruction tuning, the textual instructions $T \in D$ are tokenized as $X^l = (x_1^l, x_2^l, \dots, x_N^l)$ using the tokenizer of the backbone LLM, which is querying the MLLM to generate textual responses conditioned on the multimodal inputs,

$$\hat{y}_k \sim \pi_\theta(\cdot | X^v, X^l, y_{<k}). \quad (1)$$

Therefore, the learning objective of visual instruction-tuning for K samples is to maximize the average log-likelihood of the ground truth answer tokens $y = (y_1, y_2, \dots, y_T)$ of each sample,

$$\mathcal{L}_{vl}(\theta) = - \sum_{t=1}^T \log \pi_\theta(y_t | X^v, X^l, y_{<t}), \quad (2)$$

where multimodal instructions X^v and X^l both serve as generation conditions.

An Information Bottleneck Perspective on Visual Knowledge Forgetting. In multimodal models, the information bottleneck [39] (IB) framework provides a powerful lens to understand how representations are formed. In our setting, the IB principle seeks a representation Z that is maximally informative about the output y while discarding irrelevant details from the inputs. For an MLLM that processes visual inputs X^v and textual inputs X^l , a full IB objective might take the form:

$$\min_{\theta} \mathcal{L}_{\text{IB}}^{\text{vision}}(\theta) = -I(y; Z) + \beta I(X^v; Z). \quad (3)$$

where $I(\cdot; \cdot)$ denotes mutual information and β controls the trade-off between predictive power and compression. This formulation explicitly highlights the risk of discarding visual details when the model is optimized primarily to predict y .

Effective Rank as a Measure of Representation Richness. To quantify the information content retained in a representation, we use the effective rank metric [44]. Given a representation matrix Z whose singular values are $\{\sigma_i\}$, the effective rank is defined as:

$$\text{erank}(Z) = \exp\left(- \sum_i p_i \log p_i\right), \quad \text{with } p_i = \frac{\sigma_i}{\sum_j \sigma_j}. \quad (4)$$

This measure, based on the entropy of the singular value distribution, captures the ‘‘richness’’ or intrinsic dimensionality of Z . A higher effective rank indicates that the representation spans a larger subspace, whereas a lower effective rank implies that the representation has been overly compressed.

4 Visual Forgetting in MLLM Instruction-tuning

Building on the IB objective Eq. (3) introduced in Section 3, we examine how instruction tuning affects the richness of visual representations. Let the pre-trained MLLM induce a latent representation,

$$Z \sim p(\cdot | X^v, X^l),$$

where Z is decomposed into modality-specific components, $Z = (Z^v, Z^l)$ with Z^v captures the visual features extracted from X^v , and Z^l encapsulates the textual features from X^l . Define the *pre-trained* visual representation space as,

$$\mathcal{Z}_0^v = \{Z_\phi^v : Z \sim p_\phi(\cdot | X^v), \quad X^v \in \Omega\}.$$

During instruction tuning, the model is optimized primarily to predict the target y . As described in Eq. (3), the IB objective introduces a trade-off between retaining visual information $I(X^v; Z)$ and ensuring that Z remains predictive of y via $I(y; Z)$ [18]. In practice, however, instruction-tuning datasets are predominantly text-driven; thus, the learned visual representation Z^v receives only indirect and often weaker supervision [54].

Let the tuned model’s latent representation be $Z_\theta \sim p_\theta(\cdot | X^v, X^l)$, and denote the corresponding visual representation space by,

$$\mathcal{Z}_\theta^v = \{Z_\phi^v : Z \sim p_\theta(\cdot | X^v, X^l), \quad (X^v, X^l) \in D\},$$

where D is the instruction-tuning dataset. To measure the richness of the visual representation, we employ the effective rank metric from Eq. (4). A higher effective rank indicates that the representation spans a broader subspace, whereas a lower effective rank signals more aggressive compression.

The Visual Forgetting Problem. During instruction tuning, the visual representation undergoes significant compression as the model prioritizes textual supervision. This reduction occurs because the model effectively sacrifices part of $I(X^v; Z)$ to focus on $I(y; Z)$, thereby reducing the effective dimensionality of the visual features. As a result, the model progressively loses its ability to retain and utilize rich visual information, leading to a phenomenon we define as **visual forgetting**. Empirically, in Figure 1 we observe,

$$\text{erank}(\mathcal{Z}_\theta^v) < \text{erank}(\mathcal{Z}_0^v). \quad (5)$$

This indicates that the tuned visual representation is compressed relative to the pre-trained space, making it harder for the model to leverage visual information effectively. In RQ3 (Section 6.3), we validate such empirical observations and demonstrate that our

method helps to preserve effective ranks in the visual representation learning of MLLMs.

5 MDGD: Modality-Decoupled Gradient Regularization and Descent

Motivated by the visual forgetting problem caused by the degradation of multimodal encoding in Eq. (5), we introduce a modality-decoupling gradient regularization (MDGD) to approximate orthogonal gradients between visual understanding drift and downstream task optimization. Specifically, leveraging modality-decoupled gradients \bar{g}_θ and \bar{g}_ϕ derived from the current MLLM and a pre-trained MLLM respectively, we propose a gradient regularization term \tilde{g}_θ for more efficient multimodal instruction tuning, which promotes the alignment of downstream tasks while mitigating visual forgetting [73]. Since MDGD requires the estimation of parameter gradients, we could not directly apply parameter-efficient fine-tuning methods (e.g., LoRA [15]). Thus, we alternatively formulate the regularization as a gradient mask $M_{\tilde{g}_\theta}$, which allows efficient fine-tuning only on a subset of masked model parameters.

5.1 Modality Decoupling

Based on the information bottleneck objective in Eq. (3), the objective encourages the model to maximize $I(y; Z)$ while compressing $I(X^v; Z)$ [2, 50]. In practice, this compression may discard useful visual details, leading to visual forgetting. To mitigate such compression and preserve the pre-trained visual knowledge, we follow the KL divergence loss $D_{\text{KL}}(\mu_\phi(X^v) \parallel \pi_\theta(X^v))$ to constrain the current model's visual representation $\pi_\theta(X^v)$ to remain close to the pre-trained distribution $\mu_\phi(X^v)$, thereby preserving the mutual information $I(X^v; Z)$ that would otherwise be reduced by the compression [13, 35]. However, since MLLMs cannot directly track the distributions of image tokens, we instead introduce an auxiliary loss function

$$\mathcal{L}_v(\phi, \theta) = \|\mu(X^v|\phi) - \pi(X^v|\theta)\|_1, \quad (6)$$

which approximates the KL divergence loss [74, 76] by penalizing discrepancies between the pre-trained visual representation and that obtained during instruction tuning.

In the MLLM instruction tuning, the visual output tokens (e.g., $\{z_k^{vl}\}_{k=1}^M$) are encoded as latent representations. Such visual encoding cannot be directly supervised by any learning objective but is learned through textual gradient propagation of the negative log-likelihood loss in downstream tasks. To approximate the visual optimization direction, we derive the gradients of $\mathcal{L}_v(\phi, \theta)$ for both the pre-trained MLLM π_ϕ and the current MLLM π_θ :

$$\begin{aligned} h_\phi &= \nabla_\phi \mathcal{L}_v(\phi) = \lambda(\phi, \theta) \cdot \nabla_\phi \mu(X^v|\phi), \\ h_\theta &= \nabla_\theta \mathcal{L}_v(\theta) = -\lambda(\phi, \theta) \cdot \nabla_\theta \pi(X^v|\theta), \end{aligned}$$

where $\lambda(\phi, \theta) = \text{sign}(\mu(X^v|\phi) - \pi(X^v|\theta))$. Intuitively, when the MLLM's visual understanding drift causes visual forgetting, we

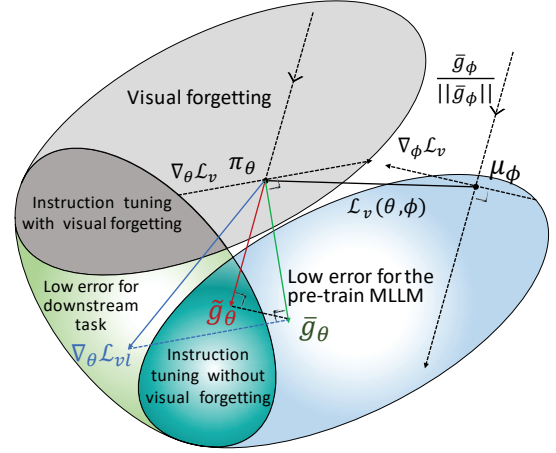


Figure 2: Illustration of the proposed method. To mitigate suboptimal optimization and prevent visual forgetting, we first project $\nabla_\theta \mathcal{L}_{vl}$ onto the direction orthogonal to $\nabla_\phi \mathcal{L}_v$, obtaining \bar{g}_θ . Next, we project \bar{g}_θ onto the direction of \bar{g}_ϕ , yielding \tilde{g}_θ . This process guides the gradient towards the optimal region without visual forgetting.

further derive the orthogonal task gradients \bar{g}_ϕ and \bar{g}_θ :

$$\bar{g}_\phi = \nabla_\phi \mathcal{L}_{vl}(\phi) - \frac{\nabla_\phi \mathcal{L}_{vl}(\phi)^\top h_\phi}{\|h_\phi\|^2} \cdot h_\phi, \quad (7)$$

$$\bar{g}_\theta = \nabla_\theta \mathcal{L}_{vl}(\theta) - \frac{\nabla_\theta \mathcal{L}_{vl}(\theta)^\top h_\theta}{\|h_\theta\|^2} \cdot h_\theta, \quad (8)$$

which enables **modality decoupling** of the downstream task gradient in Eq.(2) orthogonal to the visual understanding drift for the pretrained MLLM $\bar{g}_\phi \perp h_\phi$ and current MLLM $\bar{g}_\theta \perp h_\theta$.

Algorithm 1 MDGD: Modality Decoupled Gradients Descent

- 1: **Inputs:** Pre-trained MLLM μ_ϕ , current MLLM π_θ , instruction-tuning dataset D , and learning rate η
 - 2: **Outputs:** The optimized model weights of π_θ
 - 3: **Initialize** $\pi_\theta \leftarrow \mu_\phi$
 - 4: **for** Receive minibatch $D_i \subset D$ **do**
 - 5: Calculate $\mathcal{L}_{vl}(\phi)$ of μ_ϕ , based on Eq.(2);
 - 6: Calculate $\mathcal{L}_{vl}(\theta)$ of π_θ , based on Eq.(2);
 - 7: Extract visual encodings of $\mu(X^v|\phi)$;
 - 8: Extract visual encodings of $\pi(X^v|\theta)$;
 - 9: Calculate $\mathcal{L}_v(\phi, \theta)$, based on Eq.(6);
 - 10: Derive orthogonal task gradients \bar{g}_ϕ and \bar{g}_θ , according to Eq.(7);
 - 11: **if** Parameter-efficient fine-tuning **then**
 - 12: Calculate $M_{\tilde{g}_\theta}$, based on Eq.(11);
 - 13: Update the model following Eq.(12).
 - 14: **else**
 - 15: Calculate \tilde{g}_θ , based on Eq.(9);
 - 16: Update the model following Eq.(10).
 - 17: **end if**
 - 18: **end for**
-

5.2 Regularized Gradient Descent

The auxiliary loss in Eq. (6) preserves the visual representation at a distribution level via the feature alignment auxiliary loss in Eq. (6). However, the information bottleneck framework indicates that the gradient component compressing $I(X^v; Z)$ (i.e., $\nabla_{\theta} I(X^v; Z)$), can harm visual preservation by reducing the effective rank of the features [1, 23].

To address this compression-induced drift, we incorporate an orthogonal gradient as a regularizer. Motivated by multi-task orthogonal gradient optimization [6, 67, 75], we leverage the gradient \bar{g}_{ϕ} from the pre-trained model μ_{ϕ} , which reflects the accumulated visual drift and approximates a global orthogonal learning effect in the downstream task. We then project the current model’s gradient onto this direction:

$$\tilde{g}_{\theta} = \frac{\bar{g}_{\theta}^{\top} \bar{g}_{\phi}}{\|\bar{g}_{\phi}\|^2} \cdot \bar{g}_{\phi}. \quad (9)$$

In addition, to prevent discrepancies between the regularization and task gradients, we include the feature alignment auxiliary loss (Eq. (6)) in the overall objective. The final parameter update is:

$$\pi_{\theta} \leftarrow \pi_{\theta} - \nabla_{\theta} \mathcal{L}_{vl}(\theta) - \nabla_{\theta} \mathcal{L}_v(\theta) - \tilde{g}_{\theta}. \quad (10)$$

5.3 Enabling Parameter-efficient Fine-tuning of MDGD via Gradient Masking

Parameter-efficient fine-tuning (PEFT) methods, such as adapters [14] and LoRA [15], aim to reduce the computational cost and memory usage when fine-tuning models on downstream tasks under practical constraints [11]. However, due to the requirement of directly estimating gradient directions on the pre-trained model parameters, MDGD cannot be directly applied to these PEFT methods, which introduce additional model parameters whose gradients are separate from the original model weights.

To address this challenge, we propose a variant, MDGD-GM, by formulating the gradient regularization term in Eq. (9) as gradient masking that selects model weights with efficient gradient directions. Specifically, we define the gradient mask as

$$M_{\tilde{g}_{\theta}} = 1 \left\{ \frac{\bar{g}_{\theta}^{\top} \bar{g}_{\phi}}{\|\bar{g}_{\phi}\| \|\bar{g}_{\theta}\|} \geq T_{\alpha} \right\}, \quad (11)$$

where T_{α} is determined by a percentile α of trainable parameters with the highest similarity scores between \bar{g}_{θ} and \bar{g}_{ϕ} . Consequently, the optimization in Eq. (10) is reformulated as

$$\pi_{\theta} \leftarrow \pi_{\theta} - M_{\tilde{g}_{\theta}} \cdot (\nabla_{\theta} \mathcal{L}_{vl}(\theta) + \nabla_{\theta} \mathcal{L}_v(\theta)). \quad (12)$$

We summarize and illustrate the optimization process of MDGD and MDGD-GM in Algorithm 1.

6 Experiments

In this section, we conduct experiments on various datasets and backbone MLLMs to investigate the following research questions:

- (1) **RQ1 (Overall Performance)** Can MDGD prevent visual forgetting while improving downstream tasks?
- (2) **RQ2 (Ablation Study)** How do the visual alignment and gradient masking affect the MDGD’s performance?
- (3) **RQ3 (Representation Learning)** How does MDGD benefit effective multimodal representation learning in MLLMs?

- (4) **RQ4 (Sensitivity Study)** How does gradient masking ratio α affects the learning of MDGD?

Datasets To evaluate the effectiveness of MDGD in mitigating catastrophic forgetting, we used two models of different sizes. Our experimental design follows the settings from the work of Zhu et al. [73]. For each model, datasets were categorized into two types: **pre-trained tasks**, which assess the model’s ability to retain inherent knowledge after fine-tuning, and **fine-tuning tasks**, consisting of unseen datasets used to test adaptability. After fine-tuning, we evaluated performance on both task types to measure forgetting and generalization. Below, we detail the datasets used for each model. **LLaVA-1.5 (Vicuna-7B)** [30]: This model has 7 billion parameters. In line with Liu et al. [30], we used the following datasets:

- **Pre-trained Tasks:** VQAv2 [9], GQA [17], VizWiz [10], SQA [36], TextVQA [49], POPE [28], and MM-Bench [34].
- **Fine-tuning:** Flickr30k [66] and OKVQA [41], which were not encountered in the pre-training stage.

MiniCPM-V-2.0 [65]: This model has 2.8 billion parameters. We evaluated its performance on:

- **Pre-trained Tasks:** VizWiz, OKVQA, A-OKVQA [45], TextVQA, IconQA [37], POPE, and MM-Bench.
- **Fine-tuning:** TextCaps [48] and PathVQA [12], which were not part of its pre-training exposure.

Baselines We compare our approach against several baselines:

- **Standard Fine-Tuning.** For a fair comparison, we follow the setting of Model-Tailor [73], where LLaVA-1.5 is fine-tuned on the last 6 layers and its feature adapter, with a total of 1.2B parameters. MiniCPM is fine-tuned on the last 8 layers and its feature resampler, with 517M parameters.
- **LoRA-based Fine-Tuning** [15]. LoRA introduces low-rank matrices to update only a small subset of parameters, reducing memory consumption and computational cost. In our experiments, LLaVA-1.5 and MiniCPM are fine-tuned by modifying the query and key projection layers within the attention mechanism.
- **Model Tailor** [73]. This baseline employs a hybrid strategy that mitigates catastrophic forgetting by identifying and adjusting the most critical parameters for adaptation. It has been evaluated through experiments on multimodal large language models (MLLMs). As the method is not open source, we report only the original results of the LLaVA-1.5 experiments provided in the original paper as a baseline.

Implementation Details We use the official Huggingface implementations of the LLaVA-1.5 and the MiniCPM-V-2.0 models and their LoRA adapters. For model fine-tuning, we use BFloat16 precision for memory-efficient training. Experiments are conducted using 2 NVIDIA A100-SXM4-80GB GPUs.

6.1 Overall Performance (RQ1)

6.1.1 Larger MLLM adapts better to downstream tasks but is more prone to visual forgetting. We study the visual forgetting problem on the LLaVA-1.5 MLLM which contains 7B model parameters and report performance comparison results in Table 1. We observe that the pre-trained LLaVA enables efficient instruction tuning on target tasks, where the zero-shot performance is near

| Method | #Params | Pre-trained tasks | | | | | | Target task | Metrics | |
|---------------------|---------|-------------------|--------------|--------------|--------------|--------------|--------------|--------------|--------------|--------------|
| | | GQA | VizWiz | SQA | TextVQA | POPE | MMBench | Flickr30k | Avg | Hscore |
| Zero-shot | – | 61.94 | 50.00 | 66.80 | 58.27 | 85.90 | 64.30 | 3.5 | 55.82 | 59.86 |
| Fine-tune | 1.2B | 56.26 | 44.45 | 28.34 | 38.98 | 38.40 | 50.56 | 78.82 | 47.97 | 45.26 |
| LoRA | 29M | 17.74 | 40.63 | 5.38 | 30.48 | 2.40 | 9.55 | 64.18 | 24.33 | 20.49 |
| Model Tailor | 273M | 52.49 | 42.28 | <u>67.15</u> | 43.89 | 82.88 | 63.40 | <u>75.40</u> | 61.07 | 59.85 |
| MDGD | 1.2B | <u>67.71</u> | <u>48.18</u> | 69.05 | <u>57.32</u> | 85.12 | <u>65.43</u> | 73.47 | 66.61 | 66.03 |
| w/o visual align | 1.2B | 57.64 | 36.95 | 53.96 | 32.84 | 30.43 | 56.66 | 65.58 | 47.72 | 46.19 |
| MDGD-GM | 124M | 69.89 | 51.22 | 65.87 | 58.18 | <u>84.39</u> | 66.42 | 64.18 | <u>65.74</u> | <u>65.86</u> |

| Method | #Params | Pre-trained tasks | | | | | | Target task | Metrics | |
|---------------------|---------|-------------------|--------------|--------------|--------------|--------------|--------------|--------------|--------------|--------------|
| | | GQA | VizWiz | SQA | TextVQA | POPE | MMBench | OKVQA | Avg | Hscore |
| Zero-shot | – | 61.94 | 50.00 | 66.80 | 58.27 | 85.90 | 64.30 | 0.14 | 55.34 | 59.58 |
| Fine-tune | 1.2B | 62.98 | 40.59 | 59.84 | 48.38 | 71.42 | 51.98 | <u>69.10</u> | 57.76 | 56.79 |
| LoRA | 29M | 63.44 | 41.61 | 51.29 | 48.02 | 75.27 | 37.31 | 71.46 | 55.49 | 54.12 |
| Model Tailor | 273M | 60.39 | 46.49 | 69.51 | 54.88 | 85.44 | <u>63.32</u> | 38.10 | 59.73 | 61.48 |
| MDGD | 1.2B | 66.55 | 42.72 | 64.60 | 52.54 | <u>85.17</u> | 61.73 | 62.29 | <u>62.23</u> | <u>62.22</u> |
| w/o visual align | 1.2B | <u>66.39</u> | 39.89 | 60.19 | 52.40 | 84.92 | 62.97 | 62.39 | 61.31 | 61.22 |
| MDGD-GM | 124M | 66.02 | <u>43.97</u> | <u>67.91</u> | <u>52.80</u> | 84.70 | 63.97 | 61.04 | 62.92 | 63.07 |

Table 1: Performance on various pre-trained tasks of LLaVA-1.5 models fine-tuned on Flickr30K and OKVQA. We report the best performance for each task in a bold font while the second best performance underlined.

zero. When the model is fine-tuned on the image caption task, Flickr30K, which largely differs from the pre-trained tasks of visual question-answering, the model can learn a degraded multimodal representation, which causes visual forgetting in its projected visual representation space (in Section 4) and its average performance on pre-trained tasks drops 33.63% compared with zero-shot performance. Fine-tuning on visual question-answering task OKVQA, which is similar to the pre-trained tasks, can also cause a 13.44% performance drop, due to the limited image-text pairs existing in the downstream task, which potentially leads to MLLM’s visual understanding drift.

6.1.2 Smaller MLLM also experiences visual forgetting while limited in downstream task improvements. To validate the observation on a smaller MLLM, we report the comparison results of MiniCPM-V-2.0 with 2.8B model parameters in Table 2. We observe that compared with the LLaVA MLLM, MiniCPM suffers from less prominent visual forgetting. The average performance drop of the model limits to 6.28% and 4.25% when fine-tuning on PathVQA and TextCaps, respectively. We attribute this observation to MiniCPM learning a more compact and constrained visual representation space during pre-training, causing the visual representations of target task images to be less aligned with those of the pre-trained MLLM. Consequently, MiniCPM exhibits limited improvement in downstream tasks, as its restricted ability to acquire additional visual knowledge leads to ineffective instruction tuning.

6.1.3 MDGD prevents visual forgetting while maintaining downstream task improvements. By employing MDGD in MLLM instruction tuning, we observe the LLaVA’s average performance drop on pre-trained tasks reduces to 3.59% when fine-tuned on OKVQA and also achieves a 1.45% improvement when fine-tuned on Flickr30K, which demonstrates the efficiency of MDGD in mitigating visual

forgetting. For the smaller MLLM, MiniCPM, MDGD achieves comparable downstream task improvements with direct fine-tuning, while completely eliminating visual forgetting in the pre-trained tasks. MDGD and its variants consistently achieve the best average performance for both MLLMs, demonstrating its great potential for incremental learning on individual downstream tasks.

6.1.4 Comparison with baseline methods. In Table 1, we compare MDGD with LoRA fine-tuning and Model Tailor [73] on LLaVA-1.5, which are designed for parameter-efficient fine-tuning. We observe that LoRA fine-tuning can suffer from significant visual forgetting on Flickr30K and OKVQA. Since LoRA introduces additional representation projections in intermediate layers, the pre-trained multimodal representations can be projected into a lower-rank subspace leading to visual forgetting (in Section 4), due to the limitation of image-text pairs in the target dataset. Model Tailor is designed for MLLM anti-forgetting, which identifies “patches” of sub-model parameters significantly affected by fine-tuning on the target task. However, since the method is not specifically designed for MLLMs, the unique challenge of visual forgetting cannot be effectively mitigated while maintaining robust performance on the target task. Thus, we observe that Model Tailor’s performance is sensitive to the target task datasets (e.g., better on Flickr30K than OKVQA), whereas MDGD consistently outperforms Model Tailor in terms of both average task scores and H-scores across the two datasets. In Table 2, we also report the results of the MDGD comparison with LoRA fine-tuning on MiniCPM. We observe consistent improvements on the average task performance of MDGD when fine-tuned on PathVQA and TextCaps, especially MDGD achieves 2.43% and 1.83% on the pre-trained tasks of PathVQA and TextCaps, respectively, which demonstrates the effectiveness of MDGD in mitigating visual forgetting.

| Method | #Params | Pre-trained tasks | | | | | | | Target task | Metrics | |
|------------------|---------|-------------------|--------------|--------------|--------------|--------------|--------------|--------------|--------------|--------------|--------------|
| | | VizWiz | A-OKVQA | OKVQA | TextVQA | IconQA | POPE | MMBench | PathVQA | Avg | Hscore |
| Zero-shot | - | 55.27 | 79.39 | 64.86 | 77.98 | 79.01 | 88.93 | 70.98 | 5.44 | 65.23 | 10.04 |
| Fine-tune | 517M | 52.91 | 76.94 | 59.06 | 58.34 | 76.96 | 89.60 | 70.16 | <u>11.04</u> | 61.88 | 18.74 |
| LoRA | 35M | 52.95 | 76.24 | 64.45 | 77.18 | 77.80 | 88.08 | 67.47 | 15.03 | 64.90 | 24.41 |
| MDGD | 517M | 55.73 | 78.25 | <u>64.33</u> | <u>77.54</u> | 79.45 | 89.19 | 71.94 | 9.09 | 65.69 | 15.97 |
| w/o visual align | 517M | 54.92 | <u>78.52</u> | 64.17 | <u>77.42</u> | <u>79.37</u> | 89.10 | 70.96 | 8.49 | <u>65.37</u> | 15.03 |
| MDGD-GM | 52M | <u>55.04</u> | 78.78 | 64.31 | 77.78 | 79.10 | 88.76 | <u>70.98</u> | 5.72 | 65.06 | 10.52 |

| Method | #Params | Pre-trained tasks | | | | | | | Target task | Metrics | |
|------------------|---------|-------------------|--------------|--------------|--------------|--------------|--------------|--------------|--------------|--------------|--------------|
| | | VizWiz | A-OKVQA | OKVQA | TextVQA | IconQA | POPE | MMBench | TextCaps | Avg | Hscore |
| Zero-shot | - | 55.27 | 79.39 | 64.86 | 77.98 | 79.01 | 88.93 | 70.98 | 15.77 | 66.52 | 25.50 |
| Fine-tune | 517M | 52.03 | 77.73 | 59.16 | 67.24 | 78.67 | 88.20 | 71.42 | 33.85 | 66.04 | 44.76 |
| LoRA | 35M | 53.30 | <u>78.17</u> | <u>63.99</u> | <u>77.68</u> | 78.28 | 87.31 | 69.23 | <u>32.41</u> | 67.55 | <u>43.80</u> |
| MDGD | 517M | 55.17 | <u>78.17</u> | 63.67 | 76.08 | <u>79.40</u> | 89.11 | <u>71.58</u> | 28.90 | <u>67.76</u> | 40.52 |
| w/o visual align | 517M | 51.35 | 78.08 | 63.06 | 76.48 | 78.99 | <u>88.98</u> | 71.30 | 25.93 | 66.77 | 37.35 |
| MDGD-GM | 52M | <u>55.04</u> | 78.43 | 65.26 | 78.08 | 79.65 | 88.93 | 71.88 | 29.14 | 68.30 | 40.85 |

Table 2: Performance on various pre-trained tasks of MiniCPM-V2.5 models fine-tuned on PathVQA and TextCaps. We report the best performance for each task in a bold font while the second best performance underlined.

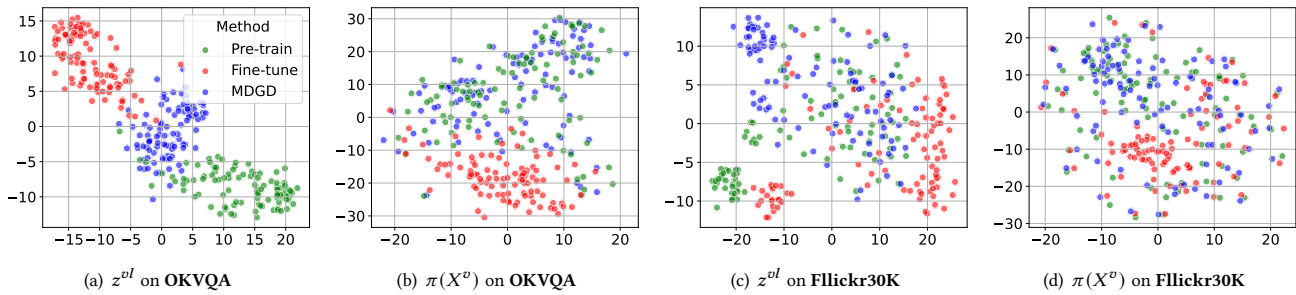


Figure 3: T-SNE plots of the distribution of extracted visual $\pi(X^v)$ and multimodal z^{vl} representations from pre-trained LLaVA-1.5, and models with direct fine-tuning and MDGD on OKVQA and Flickr30K.

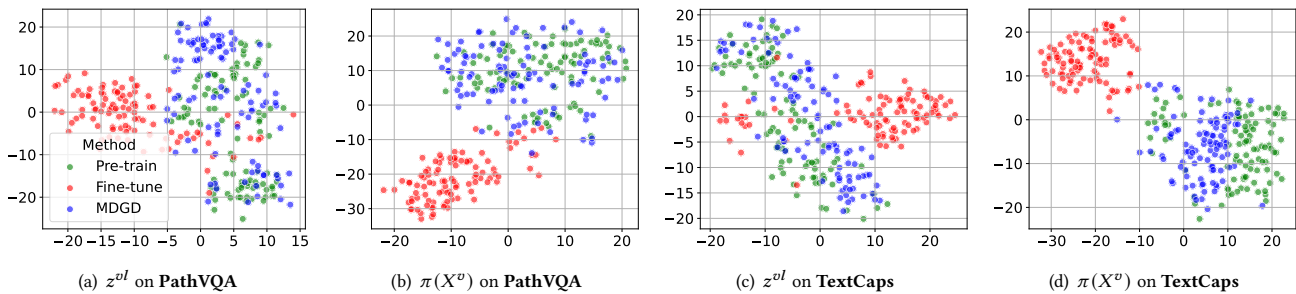


Figure 4: T-SNE plots of the distribution of extracted visual $\pi(X^v)$ and multimodal z^{vl} representations from pre-trained MiniCPM, and models with direct fine-tuning and MDGD on PathVQA and TextCaps.

6.2 Ablation Study (RQ2)

6.2.1 Ablation study on visual alignment. We compare MDGD with its two variants, MDGD w/o visual align and MDGD-GM. MDGD w/o visual align enables MDGD without including visual representation loss $\mathcal{L}_v(\phi, \theta)$ Eq.(6), to understand the effect of directly optimizing to reduce the visual representation discrepancy between

the current model and pre-trained model. We observe that MDGD w/o visual align maintains relatively comparable performance to MDGD on OKVQA and PathQA, due to the reduced need for visual representation adaptation in such visual question-answering tasks. In contrast, tasks like image captioning on Flickr30K and TextCaps

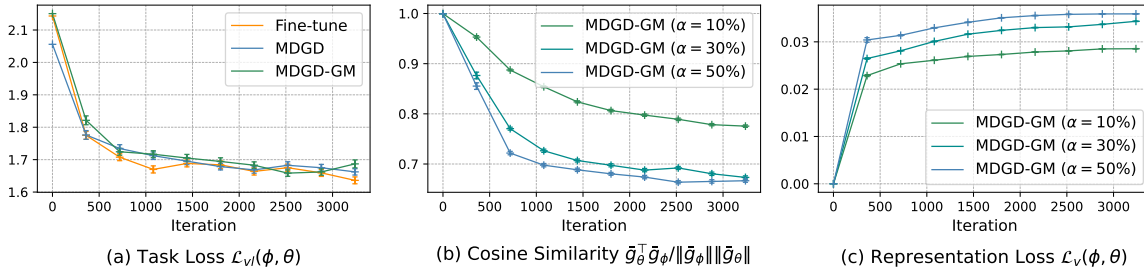


Figure 5: Illustration of (a) the learning process of three methods based on task loss $\mathcal{L}_{ol}(\phi, \theta)$, (b) the average regularized cosine similarity $\frac{\bar{g}_\theta^T \bar{g}_\phi}{\|\bar{g}_\theta\| \|\bar{g}_\phi\|}$ in Eq.(11) for gradient masking at varying ratios, and (c) the visual representation loss $\mathcal{L}_v(\phi, \theta)$ in Eq.(6) for gradient masking at varying ratios α .

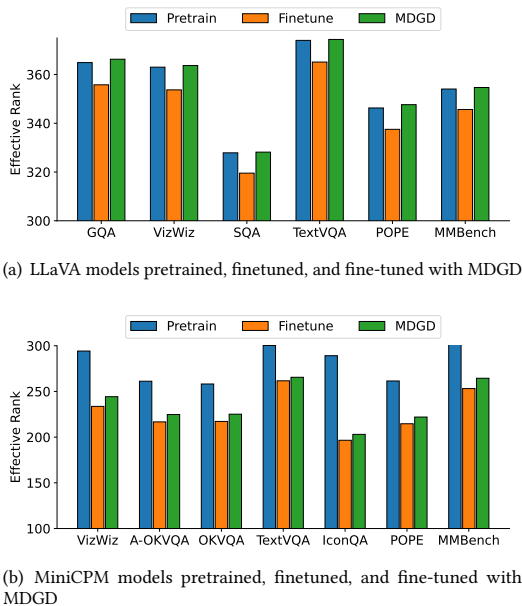


Figure 6: The effective rank comparison on individual downstream fine-tuning datasets.

benefit from feature alignment regularization, which directly mitigates visual understanding drift in the MLLM.

6.2.2 Ablation study on gradient masking. The other variant, MDGD-GM, leverages gradient masking to enable parameter-efficient fine-tuning (PEFT). We observe the PEFT variant of MDGD consistently achieves comparable performance across all tasks and backbone MLLMs, which only fine-tunes a subset of 10% original MLLM parameters used for direct fine-tuning and original MDGD. Different from conventional PEFT methods such as adapters, MDGD and its variants do not introduce additional parameters to the original model architecture, enabling continuous and incremental learning in an online setting [8, 40].

6.3 Representation Study (RQ3)

6.3.1 T-SNE Analysis on Visual Representation. To analyze the learning of visual and multimodal representation distributions in

MLLMs, we create T-SNE [53] plots to visualize the feature distributions extracted from pre-trained MLLMs, as well as MLLMs after standard fine-tuning and MDGD. We illustrate the distributions of the multimodal features z^{vl} extracted from the last token of the multimodal instruction tokens, and the visual features $\pi_\theta(X^v)$ extracted from the last token of the input image tokens. We observe a consistent visual understanding drift in the MLLMs’ visual representation spaces after standard fine-tuning on Flickr30K and OKVQA with LLaVA (Figure 3b and 3d), as well as PathVQA and TextCaps with MiniCPM (Figure 4b and 4d). By employing MDGD to mitigate visual forgetting, we observe that visual understanding drift is effectively reduced, allowing the fine-tuned MLLM to retain pre-trained visual capabilities and preserve visual information.

We further observe a distributional discrepancy in the multimodal representation z^{vl} of LLaVA (Figures 3a and 3c) between MDGD and the pre-trained MLLM. This discrepancy arises from the alignment of the MLLM to the target task through multimodal instructions, demonstrating effective adaptation to the downstream task of the LLaVA model. In addition, we also observe such multimodal distribution discrepancy reduces in a smaller MLLM, MiniCPM. This observation aligns with our findings on MiniCPM in Section 6.1, where we noted limited effects in model adaptation to downstream tasks. However, applying MDGD to MiniCPM mitigates visual forgetting by preventing degradation of both image and multimodal encodings into lower-rank representation spaces.

6.3.2 Effective Rank Analysis on Visual Representation. To quantitatively analyze the visual forgetting problem (in Section 4) described in Eq. (5), we calculate effective ranks of the visual representations extracted from the last hidden layer on the position of image tokens in individual MLLMs. We show the comparison results of LLaVA models in Figure 6(a) and MiniCPM models in Figure 6(b). We observe that with both the backbone models of LLaVA and MiniCPM, directly fine-tuning the pre-trained models on downstream tasks can lead to a consistent reduction of effective ranks in visual representations. Such observations validate the hypothesis in Section 4 regarding the potential visual forgetting problem in MLLM instruction tuning. In addition, we can observe that MDGD achieves consistent improvements in effective ranks compared with the standard fine-tuning method for both backbone MLLMs across various pre-trained tasks. In Figure 6(a), we observe that MDGD achieves comparable or even better effective ranks on pre-trained tasks, compared with the pre-trained LLaVA model.

However, MDGD on MiniCPM in Figure 6(b) also suffers from the visual representation degradation problem, while MDGD consistently alleviates the problem. Such observation suggests a higher risk of visual forgetting in smaller-scale MLLMs.

6.4 Sensitivity Study (RQ4)

We evaluate the learning curves of MDGD and MDGD-GM compared with standard fine-tuning in Figure 5(a), where we observe that MDGD and MDGD-GM achieve comparable training efficiency compared with the standard fine-tuning method. We also investigate the sensitivity of gradient cosine similarity between \bar{g}_θ and \bar{g}_ϕ in Figure 5(b) and the representation loss in Figure 5(c), with respect to the gradient masking ratio in MDGD-GM. In Figure 5(b), we observe that MDGD-GM with lower gradient masking ratios can better align the modality-decoupled learning gradients between the target model and the pre-trained model, while MDGD-GM maintains over 70% alignment with 50% gradient masking. In Figure 5(c), we show that MDGD-GM with 50% gradient masking still effectively alleviates the visual representation degradation problem by reducing the visual representation discrepancy \mathcal{L}_v , while learning with a more active gradient can achieve better alignment.

7 Conclusion

In this work, we addressed the challenge of visual forgetting in MLLMs during instruction tuning by introducing a novel modality-decoupled gradient descent (MDGD) approach. MDGD disentangles the gradient updates for visual representation learning from task-specific alignment, thereby preserving the effective rank of pre-trained visual features and mitigating the over-compression effects highlighted by the information bottleneck perspective. This decoupling enables MLLMs to retain rich visual knowledge while adapting robustly to new downstream tasks. Furthermore, our gradient masking variant, MDGD-GM, enhances memory efficiency and optimizes parameter usage, making fine-tuning both practical and scalable. Extensive experiments across various downstream tasks and backbone models demonstrate that MDGD not only effectively prevents visual forgetting but also outperforms existing strategies in achieving balanced multimodal representation learning and task adaptation. Our findings underscore the importance of preserving visual representations during instruction-tuning and offer a viable solution for efficient and effective multimodal learning in real-world scenarios.

References

- [1] Alessandro Achille and Stefano Soatto. 2018. Information dropout: Learning optimal representations through noisy computation. *IEEE transactions on pattern analysis and machine intelligence* 40, 12 (2018), 2897–2905.
- [2] Alexander A Alemi, Ian Fischer, Joshua V Dillon, and Kevin Murphy. 2016. Deep variational information bottleneck. *arXiv preprint arXiv:1612.00410* (2016).
- [3] Jinze Bai, Shuai Bai, Shusheng Yang, Shijie Wang, Sinan Tan, Peng Wang, Junyang Lin, Chang Zhou, and Jingren Zhou. 2023. Qwen-vl: A frontier large vision-language model with versatile abilities. *arXiv preprint arXiv:2308.12966* (2023).
- [4] Zechen Bai, Pichao Wang, Tianjun Xiao, Tong He, Zongbo Han, Zheng Zhang, and Mike Zheng Shou. 2024. Hallucination of multimodal large language models: A survey. *arXiv preprint arXiv:2404.18930* (2024).
- [5] Grégoire Delétang, Anian Ruoss, Paul-Ambroise Duquenne, Elliot Catt, Tim Genewein, Christopher Mattern, Jordi Grau-Moya, Li Kevin Wenliang, Matthew Aitchison, Laurent Orseau, et al. 2023. Language modeling is compression. *arXiv preprint arXiv:2309.10668* (2023).
- [6] Xin Dong, Ruizhe Wu, Chao Xiong, Hai Li, Lei Cheng, Yong He, Shiyu Qian, Jian Cao, and Linjian Mo. 2022. GDOD: Effective Gradient Descent using Orthogonal Decomposition for Multi-Task Learning. In *Proceedings of the 31st ACM International Conference on Information & Knowledge Management*. 386–395.
- [7] Muhammad Fawi. 2024. CURLoRA: Stable LLM Continual Fine-Tuning and Catastrophic Forgetting Mitigation. *arXiv preprint arXiv:2408.14572* (2024).
- [8] Peng Gao, Jiaming Han, Renrui Zhang, Ziyi Lin, Shijie Geng, Aojun Zhou, Wei Zhang, Pan Lu, Conghui He, Xiangyu Yue, et al. 2023. Llama-adapter v2: Parameter-efficient visual instruction model. *arXiv preprint arXiv:2304.15010* (2023).
- [9] Yash Goyal, Tejas Khot, Douglas Summers-Stay, Dhruv Batra, and Devi Parikh. 2017. Making the v in vqa matter: Elevating the role of image understanding in visual question answering. In *Proceedings of the IEEE conference on computer vision and pattern recognition*. 6904–6913.
- [10] Danna Gurari, Qing Li, Abigale J Stangl, Anhong Guo, Chi Lin, Kristen Grauman, Jiebo Luo, and Jeffrey P Bigham. 2018. Vizwiz grand challenge: Answering visual questions from blind people. In *Proceedings of the IEEE conference on computer vision and pattern recognition*. 3608–3617.
- [11] Zeyu Han, Chao Gao, Jinyang Liu, Sai Qian Zhang, et al. 2024. Parameter-efficient fine-tuning for large models: A comprehensive survey. *arXiv preprint arXiv:2403.14608* (2024).
- [12] Xuehai He, Yichen Zhang, Luntian Mou, Eric Xing, and Pengtao Xie. 2020. PathVQA: 30000+ Questions for Medical Visual Question Answering. *arXiv preprint arXiv:2003.10286* (2020).
- [13] Geoffrey Hinton. 2015. Distilling the Knowledge in a Neural Network. *arXiv preprint arXiv:1503.02531* (2015).
- [14] Neil Houlsby, Andrei Giurgiu, Stanislaw Jastrzebski, Bruna Morrone, Quentin De Laroussilhe, Andrea Gesmundo, Mona Attariyan, and Sylvain Gelly. 2019. Parameter-efficient transfer learning for NLP. In *International conference on machine learning*. PMLR, 2790–2799.
- [15] Edward J Hu, Yelong Shen, Phillip Wallis, Zeyuan Allen-Zhu, Yuanzhi Li, Shean Wang, Lu Wang, and Weizhu Chen. 2021. Lora: Low-rank adaptation of large language models. *arXiv preprint arXiv:2106.09685* (2021).
- [16] Wen Huang, Hongbin Liu, Minxin Guo, and Neil Zhenqiang Gong. 2024. Visual hallucinations of multi-modal large language models. *arXiv preprint arXiv:2402.14683* (2024).
- [17] Drew A Hudson and Christopher D Manning. 2019. Gqa: A new dataset for real-world visual reasoning and compositional question answering. In *Proceedings of the IEEE/CVF conference on computer vision and pattern recognition*. 6700–6709.
- [18] Jingjing Jiang, Ziyi Liu, and Nanning Zheng. 2024. Correlation information bottleneck: Towards adapting pretrained multimodal models for robust visual question answering. *International Journal of Computer Vision* 132, 1 (2024), 185–207.
- [19] Wenyuan Jiang, Wenwei Wu, Le Zhang, Zixuan Yuan, Jian Xiang, Jingbo Zhou, and Hui Xiong. 2024. Killing Two Birds with One Stone: Cross-modal Reinforced Prompting for Graph and Language Tasks. In *Proceedings of the 30th ACM SIGKDD Conference on Knowledge Discovery and Data Mining*. 1301–1312.
- [20] Zhiying Jiang, Raphael Tang, Ji Xin, and Jimmy Lin. 2020. Inserting information bottlenecks for attribution in transformers. *arXiv preprint arXiv:2012.13838* (2020).
- [21] Congyun Jin, Ming Zhang, Weixiao Ma, Yujiao Li, Yingbo Wang, Yabo Jia, Yuliang Du, Tao Sun, Haowen Wang, Cong Fan, et al. 2024. RJUA-MedDQA: A Multimodal Benchmark for Medical Document Question Answering and Clinical Reasoning. In *Proceedings of the 30th ACM SIGKDD Conference on Knowledge Discovery and Data Mining*. 5218–5229.
- [22] Dohwan Ko, Ji Soo Lee, Wooyoung Kang, Byungseok Roh, and Hyunwoo J Kim. 2023. Large language models are temporal and causal reasoners for video question answering. *arXiv preprint arXiv:2310.15747* (2023).
- [23] Kuang-Huei Lee, Anurag Arnab, Sergio Guadarrama, John Canny, and Ian Fischer. 2021. Compressive visual representations. *Advances in Neural Information Processing Systems* 34 (2021), 19538–19552.
- [24] Chen Li, Yixiao Ge, Dian Li, and Ying Shan. 2024. Vision-language instruction tuning: A review and analysis. *Transactions on Machine Learning Research* (2024).
- [25] Junnan Li, Dongxu Li, Silvio Savarese, and Steven Hoi. 2023. Blip-2: Bootstrapping language-image pre-training with frozen image encoders and large language models. In *International conference on machine learning*. PMLR, 19730–19742.
- [26] Juncheng Li, Kaihang Pan, Zhiqi Ge, Minghe Gao, Wei Ji, Wenqiao Zhang, Tat-Seng Chua, Siliang Tang, Hanwang Zhang, and Yueting Zhuang. 2023. Fine-tuning multimodal llms to follow zero-shot demonstrative instructions. In *The Twelfth International Conference on Learning Representations*.
- [27] Qintong Li, Zhiyong Wu, Lingpeng Kong, and Wei Bi. 2022. Explanation regeneration via information bottleneck. *arXiv preprint arXiv:2212.09603* (2022).
- [28] Yifan Li, Yifan Du, Kun Zhou, Jinpeng Wang, Wayne Xin Zhao, and Ji-Rong Wen. 2023. Evaluating object hallucination in large vision-language models. *arXiv preprint arXiv:2305.10355* (2023).
- [29] Zhenqing Ling, Daoyuan Chen, Liuyi Yao, Yaliang Li, and Ying Shen. 2024. On the convergence of zeroth-order federated tuning for large language models. In *Proceedings of the 30th ACM SIGKDD Conference on Knowledge Discovery and Data Mining*. 1827–1838.

- [30] Haotian Liu, Chunyuan Li, Yuheng Li, and Yong Jae Lee. 2024. Improved baselines with visual instruction tuning. In *Proceedings of the IEEE/CVF Conference on Computer Vision and Pattern Recognition*. 26296–26306.
- [31] Haotian Liu, Chunyuan Li, Qingyang Wu, and Yong Jae Lee. 2024. Visual instruction tuning. *Advances in neural information processing systems* 36 (2024).
- [32] Jialin Liu, Jianhua Wu, Jie Liu, and Yutai Duan. 2024. Learning Attentional Mixture of LoRAs for Language Model Continual Learning. *arXiv preprint arXiv:2409.19611* (2024).
- [33] Qijiong Liu, Jieming Zhu, Yanting Yang, Quanyu Dai, Zhaocheng Du, Xiao-Ming Wu, Zhou Zhao, Rui Zhang, and Zhenhua Dong. 2024. Multimodal pretraining, adaptation, and generation for recommendation: A survey. In *Proceedings of the 30th ACM SIGKDD Conference on Knowledge Discovery and Data Mining*. 6566–6576.
- [34] Yuan Liu, Haodong Duan, Yuanhan Zhang, Bo Li, Songyang Zhang, Wangbo Zhao, Yike Yuan, Jiaqi Wang, Conghui He, Ziwei Liu, et al. 2023. Mmbench: Is your multi-modal model an all-around player? *arXiv preprint arXiv:2307.06281* (2023).
- [35] Román López, Jeffrey Regier, Michael I Jordan, and Nir Yosef. 2018. Information constraints on auto-encoding variational bayes. *Advances in neural information processing systems* 31 (2018).
- [36] Pan Lu, Swaroop Mishra, Tanglin Xia, Liang Qiu, Kai-Wei Chang, Song-Chun Zhu, Oyvind Tafjord, Peter Clark, and Ashwin Kalyan. 2022. Learn to explain: Multimodal reasoning via thought chains for science question answering. *Advances in Neural Information Processing Systems* 35 (2022), 2507–2521.
- [37] Pan Lu, Liang Qiu, Jiaqi Chen, Tony Xia, Yizhou Zhao, Wei Zhang, Zhou Yu, Xiaodan Liang, and Song-Chun Zhu. 2021. IconQA: A New Benchmark for Abstract Diagram Understanding and Visual Language Reasoning. In *The 35th Conference on Neural Information Processing Systems (NeurIPS) Track on Datasets and Benchmarks*.
- [38] Yun Luo, Zhen Yang, Fandong Meng, Yafu Li, Jie Zhou, and Yue Zhang. 2023. An empirical study of catastrophic forgetting in large language models during continual fine-tuning. *arXiv preprint arXiv:2308.08747* (2023).
- [39] Sijie Mai, Ying Zeng, and Haifeng Hu. 2022. Multimodal information bottleneck: Learning minimal sufficient unimodal and multimodal representations. *IEEE Transactions on Multimedia* 25 (2022), 4121–4134.
- [40] Davide Maltoni and Vincenzo Lomonaco. 2019. Continuous learning in single-incremental-task scenarios. *Neural Networks* 116 (2019), 56–73.
- [41] Kenneth Marino, Mohammad Rastegari, Ali Farhadi, and Roozbeh Mottaghi. 2019. Ok-vqa: A visual question answering benchmark requiring external knowledge. In *Proceedings of the IEEE/cvf conference on computer vision and pattern recognition*. 3195–3204.
- [42] Qian Niu, Keyu Chen, Ming Li, Pohsun Feng, Ziqian Bi, Junyu Liu, and Benji Peng. 2024. From Text to Multimodality: Exploring the Evolution and Impact of Large Language Models in Medical Practice. *arXiv preprint arXiv:2410.01812* (2024).
- [43] Artemis Panagopoulou, Le Xue, Ning Yu, Junnan Li, Dongxu Li, Shafiq Joty, Ran Xu, Silvio Savarese, Caiming Xiong, and Juan Carlos Niebles. 2023. X-instructblip: A framework for aligning x-modal instruction-aware representations to llms and emergent cross-modal reasoning. *arXiv preprint arXiv:2311.18799* (2023).
- [44] Olivier Roy and Martin Vetterli. 2007. The effective rank: A measure of effective dimensionality. In *2007 15th European signal processing conference*. IEEE, 606–610.
- [45] Dustin Schwenk, Apoorv Khandelwal, Christopher Clark, Kenneth Marino, and Roozbeh Mottaghi. 2022. A-okvqa: A benchmark for visual question answering using world knowledge. In *European conference on computer vision*. Springer, 146–162.
- [46] Ashish Shenoy, Yichao Lu, Srihari Jayakumar, Debojeet Chatterjee, Mohsen Moslehpour, Pierce Chuang, Abhay Harpale, Vikas Bhardwaj, Di Xu, Shicong Zhao, et al. 2024. Lumos: Empowering multimodal llms with scene text recognition. In *Proceedings of the 30th ACM SIGKDD Conference on Knowledge Discovery and Data Mining*. 5690–5700.
- [47] Haizhou Shi, Zihao Xu, Hengyi Wang, Weiyei Qin, Wenyuan Wang, Yibin Wang, and Hao Wang. 2024. Continual learning of large language models: A comprehensive survey. *arXiv preprint arXiv:2404.16789* (2024).
- [48] Oleg Sidorov, Ronghang Hu, Marcus Rohrbach, and Amanpreet Singh. 2020. Textcaps: a dataset for image captioning with reading comprehension. In *Computer Vision—ECCV 2020: 16th European Conference, Glasgow, UK, August 23–28, 2020, Proceedings, Part II* 16. Springer, 742–758.
- [49] Amanpreet Singh, Vivek Natarajan, Meet Shah, Yu Jiang, Xinlei Chen, Dhruv Batra, Devi Parikh, and Marcus Rohrbach. 2019. Towards vqa models that can read. In *Proceedings of the IEEE/CVF conference on computer vision and pattern recognition*. 8317–8326.
- [50] Naftali Tishby, Fernando C Pereira, and William Bialek. 2000. The information bottleneck method. *arXiv preprint physics/0004057* (2000).
- [51] Yu-Hsiang Tseng, Pin-Er Chen, Da-Chen Lian, and Shu-Kai Hsieh. 2024. The Semantic Relations in LLMs: An Information-theoretic Compression Approach. In *Proceedings of the Workshop: Bridging Neurons and Symbols for Natural Language Processing and Knowledge Graphs Reasoning (NeusymBridge)@ LREC-COLING-2024*. 8–21.
- [52] Chandra Shekhara Kaushik Valmeekam, Krishna Narayanan, Dileep Kalathil, Jean-Francois Chamberland, and Srinivas Shakkottai. 2023. Llmzip: Lossless text compression using large language models. *arXiv preprint arXiv:2306.04050* (2023).
- [53] Laurens Van der Maaten and Geoffrey Hinton. 2008. Visualizing data using t-SNE. *Journal of machine learning research* 9, 11 (2008).
- [54] Fei Wang, Wenxuan Zhou, James Y Huang, Nan Xu, Sheng Zhang, Hoifung Poon, and Muhao Chen. 2024. mDPO: Conditional Preference Optimization for Multimodal Large Language Models. *arXiv preprint arXiv:2406.11839* (2024).
- [55] Xiao Wang, Tianze Chen, Qiming Ge, Han Xia, Rong Bao, Rui Zheng, Qi Zhang, Tao Gui, and Xuanjing Huang. 2023. Orthogonal subspace learning for language model continual learning. *arXiv preprint arXiv:2310.14152* (2023).
- [56] Lai Wei, Zhiqian Tan, Chenghai Li, Jindong Wang, and Weiran Huang. 2024. Diff-eRank: A Novel Rank-Based Metric for Evaluating Large Language Models. In *The Thirty-eighth Annual Conference on Neural Information Processing Systems*.
- [57] Junda Wu, Xintong Li, Tong Yu, Yu Wang, Xiang Chen, Jiuxiang Gu, Lina Yao, Jingbo Shang, and Julian McAuley. 2024. Commit: Coordinated instruction tuning for multimodal large language models. *arXiv preprint arXiv:2407.20454* (2024).
- [58] Junda Wu, Hanjia Lyu, Yu Xia, Zhehao Zhang, Joe Barrow, Ishita Kumar, Mehrnoosh Mirtaheri, Hongjie Chen, Ryan A Rossi, Franck Dernoncourt, et al. 2024. Personalized Multimodal Large Language Models: A Survey. *arXiv preprint arXiv:2412.02142* (2024).
- [59] Junda Wu, Rui Wang, Tong Yu, Ruiyi Zhang, Handong Zhao, Shuai Li, Ricardo Henao, and Ani Nenkova. 2022. Context-aware information-theoretic causal de-biasing for interactive sequence labeling. In *Findings of the Association for Computational Linguistics: EMNLP 2022*. 3436–3448.
- [60] Junda Wu, Tong Yu, Rui Wang, Zhao Song, Ruiyi Zhang, Handong Zhao, Chaochao Lu, Shuai Li, and Ricardo Henao. 2024. Infoprompt: Information-theoretic soft prompt tuning for natural language understanding. *Advances in Neural Information Processing Systems* 36 (2024).
- [61] Junda Wu, Zhehao Zhang, Yu Xia, Xintong Li, Zhaoyang Xia, Aaron Chang, Tong Yu, Sungchul Kim, Ryan A Rossi, Ruiyi Zhang, et al. 2024. Visual prompting in multimodal large language models: A survey. *arXiv preprint arXiv:2409.15310* (2024).
- [62] Tongtong Wu, Linhao Luo, Yuan-Fang Li, Shirui Pan, Thuy-Trang Vu, and Ghulamreza Haffari. 2024. Continual learning for large language models: A survey. *arXiv preprint arXiv:2402.01364* (2024).
- [63] An Yan, Zhengyuan Yang, Junda Wu, Wanrong Zhu, Jianwei Yang, Linjie Li, Kevin Lin, Jianfeng Wang, Julian McAuley, Jianfeng Gao, et al. 2024. List Items One by One: A New Data Source and Learning Paradigm for Multimodal LLMs. *arXiv preprint arXiv:2404.16375* (2024).
- [64] Zhou Yang, Zhengyu Qi, Zhaochun Ren, Zhikai Jia, Haizhou Sun, Xiaofei Zhu, and Xiangwen Liao. 2025. Exploring Information Processing in Large Language Models: Insights from Information Bottleneck Theory. *arXiv preprint arXiv:2501.00999* (2025).
- [65] Yuan Yao, Tianyu Yu, Ao Zhang, Chongyi Wang, Junbo Cui, Hongji Zhu, Tianchi Cai, Haoyu Li, Weilin Zhao, Zhihui He, Qianyu Chen, Huarong Zhou, Zhensheng Zou, Haoye Zhang, Shengding Hu, Zhi Zhang, Jie Zhou, Jie Cai, Xu Han, Guoyang Zeng, Dahai Li, Zhiyuan Liu, and Maosong Sun. 2024. MiniCPM-V: A GPT-4V Level MLLM on Your Phone. *arXiv preprint arXiv:2408.01800* (2024). <https://arxiv.org/abs/2408.01800>
- [66] Peter Young, Alice Lai, Micah Hodosh, and Julia Hockenmaier. 2014. From image descriptions to visual denotations: New similarity metrics for semantic inference over event descriptions. *Transactions of the Association for Computational Linguistics* 2 (2014), 67–78.
- [67] Tianhe Yu, Saurabh Kumar, Abhishek Gupta, Sergey Levine, Karol Hausman, and Chelsea Finn. 2020. Gradient surgery for multi-task learning. *arXiv preprint arXiv:2001.06782* (2020).
- [68] Yuexiang Zhai, Shengbang Tong, Xiao Li, Mu Cai, Qing Qu, Yong Jae Lee, and Yi Ma. 2023. Investigating the catastrophic forgetting in multimodal large language models. *arXiv preprint arXiv:2309.10313* (2023).
- [69] Cenyuan Zhang, Xiang Zhou, Yixin Wan, Xiaoqing Zheng, Kai-Wei Chang, and Cho-Jui Hsieh. 2022. Improving the adversarial robustness of NLP models by information bottleneck. *arXiv preprint arXiv:2206.05511* (2022).
- [70] Yipeng Zhang, Xin Wang, Hong Chen, Jiawei Fan, Weigao Wen, Hui Xue, Hong Mei, and Wenwu Zhu. 2024. Large Language Model with Curriculum Reasoning for Visual Concept Recognition. In *Proceedings of the 30th ACM SIGKDD Conference on Knowledge Discovery and Data Mining*. 6269–6280.
- [71] Junhao Zheng, Qianli Ma, Zhen Liu, Binquan Wu, and Huawen Feng. 2024. Beyond Anti-Forgetting: Multimodal Continual Instruction Tuning with Positive Forward Transfer. *arXiv preprint arXiv:2401.09181* (2024).
- [72] Guanyu Zhou, Yibo Yan, Xin Zou, Kun Wang, Aiwei Liu, and Xuming Hu. 2024. Mitigating Modality Prior-Induced Hallucinations in Multimodal Large Language Models via Deciphering Attention Causality. *arXiv preprint arXiv:2410.04780* (2024).
- [73] Didi Zhu, Zhongyi Sun, Zexi Li, Tao Shen, Ke Yan, Shouhong Ding, Kun Kuang, and Chao Wu. 2024. Model Tailor: Mitigating Catastrophic Forgetting in Multimodal Large Language Models. *arXiv preprint arXiv:2402.12048* (2024).

- [74] Jun-Yan Zhu, Taesung Park, Phillip Isola, and Alexei A Efros. 2017. Unpaired image-to-image translation using cycle-consistent adversarial networks. In *Proceedings of the IEEE international conference on computer vision*. 2223–2232.
- [75] Shijie Zhu, Hui Zhao, Pengjie Wang, Hongbo Deng, Jian Xu, and Bo Zheng. 2022. Gradient deconfliction via orthogonal projections onto subspaces for multi-task learning. (2022).
- [76] Xianchao Zhu, Tianyi Huang, Ruiyuan Zhang, and William Zhu. 2022. WDIBS: Wasserstein deterministic information bottleneck for state abstraction to balance state-compression and performance. *Applied Intelligence* (2022), 1–14.